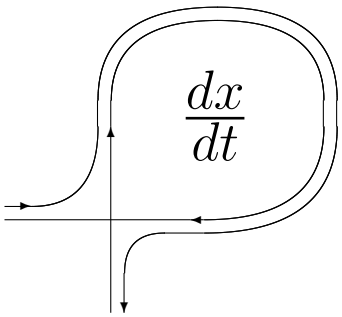

DIFFERENTIAL EQUATIONS
AND
CONTROL PROCESSES
N 1, 2007
Electronic Journal,
reg. N P2375 at 07.03.97
ISSN 1817-2172

http://www.neva.ru/journal
http://www.math.spbu.ru/user/diffjournal/
e-mail: jodiff@mail.ru

Computer software for the investigation
of differential equations, dynamical systems, and control processes

ON THE DIGITAL VISUALIZATION OF HEDGEHOGS IN HOLOMORPHIC DYNAMICS

Alessandro Rosa

Freelance programmer
c/o Locatelli,
Via Cappuccini 116/A,
I-72100 Brindisi, Italy
e-mail: zandor_zz@yahoo.it

Abstract

In the field of holomorphic dynamics in one complex variable, the 'hedgehog' is the local and invariant set arising around irrationally indifferent fixed point with a small or empty local linearization domain. Endowed with a very complicate shape, its existence depends upon weak numerical conditions and the problem of its digital visualization is open. We give an approach enjoying a far-reaching insight and crunching the long computation times, as required by other graphical methods.

1 Introduction

Let $\mathbb{C}$ be the complex plane. Since ∞ cannot be handled like an ordinary point, the compactification $\mathbb{C}_\infty \equiv \mathbb{C} \cup \{\infty\}$ turns $\mathbb{C}$ into the so–called *extended* complex

plane. Anyway the visual representation of the neighborhood of ∞ is still impracticable; Riemann cracked this problem by the stereographic projection of $\mathbb{C}_\infty$ onto a sphere model, usually of unit diameter: namely, the *Riemann sphere* $\hat{\mathbb{C}}$.

Under the term 'holomorphic dynamics' (or 'complex dynamics'), one collects the studies on the sequences of points generated by the families of functions $f_n(z)$, where $f(z) : \mathbb{C}_\infty^v \to \mathbb{C}_\infty^v, z \in \mathbb{C}_\infty^v$, in the backward and forward sense:

$$f_{-n} \equiv f_{-1}[f_{(-n+1)}], \ldots, f_{-2} \equiv f_{-1}[f_{-1}]$$

$$f_0 \equiv z,$$

$$f_1 \equiv f, f_2 \equiv f_1[f_1], \ldots, \ f_n \equiv f[f_{(n-1)}],$$

depending if $n < 0$ and $n \geq 0$ respectively. The function f is non-linear and of finite degree, of given kind (entire, meromorphic, transcendental, permutable, ...), in one or several complex variables (depending on $v \geq 1$). Given a starting point $z_0 \in \mathbb{C}_\infty^v$ (the *seed*), the sequence of points $z_n = f_n(z)$, generated by the family along both senses, is termed 'orbit'.

Since Arthur Cayley's works in 1879–80 on the Newton-Raphson iterative method [7, 8, 9], together with Schröder's [27, 28] and Koenigs' seminal results [14, 15, 16], it was clear that the fate of forward orbits is susceptible to changes either topologically, according to the seed z_0 location, and algebraically because it is locally characterized by the linear term of $f(z)$ or of its Taylorian expansion. The natural development path was to catch a new perspective for understanding the orbits behavior all over $\hat{\mathbb{C}}$; this was accomplished via the classification of invariant features (or *invariants*, for short), i.e. of entities (of any nature) which do not change under the (iterated) application of the function $f(z)$. One may speak of local or of global geometrical invariants, if they extend in a bounded domain $X \subset \mathbb{C}_\infty^v$ or not, when $X \equiv \mathbb{C}_\infty^v$.

We will focus on the holomorphic dynamics in one complex variable ($v = 1$), representing the most prolific trend in research terms today. The related history features periods of strong interest alternating to intervals of apathy for the subject: last century events tell that it drastically developed as local investigations extended to global scope, when $\mathbb{C}_\infty^1$ was assumed as the maximal domain of investigation. A first and comfortable envision of this field may come out from splitting (only theoretically) the '*local*' results from '*global*' ones. These two branches are only conceptually disjoint, in fact one branch results can be applied to the other: nevertheless the fate of (inverse and forward[1]) orbits is susceptible to changes either topologically, according to the seed z_0 location, and algebraically because it is locally characterized by the linear term of $f(z)$ or of its Taylorian expansion. The natural development path was to catch a new perspective for understanding the orbits behavior all over $\hat{\mathbb{C}}$; this was accomplished via the classification of invariant features (or *invariants*, for short), i.e. of entities (of any nature) which do not change under the (iterated) application of the function $f(z)$. One may speak of local or of global geometrical invariants, if they extend in a bounded domain $X \subset \mathbb{C}_\infty^v$ or not, when $X \equiv \mathbb{C}_\infty^v$.

[1]Whether the iterative index n is negative or positive respectively.

orbits closely relates, locally and globally, to the nature of the fixed point δ and its neighborhood.

Topologically, the dynamics in one complex variable could approach to limit invariants up to dimension (dim) 2 at most: points (dim 0), lines (dim 1) or surfaces (dim 2). Again, they could include finitely and of infinitely many points (dim 0); or be a continuum (dim 1 and 2). The union of invariants with the same properties is the *invariant set*. The goal of holomorphic dynamics is to understand the structure and role of such invariant sets by the algebraic, topological, geometrical and, in some particular cases, from the numerical viewpoint too. And coming along that way, some advanced questions arise to high degrees of complication, even deserving a multilateral attack via Complex Analysis, Topology, Theory of Numbers, Uniformization Theory.

Invariants including finitely many points of order $k > 1$ are said *limit cycles of periodic points* δ_n:

$$f(\delta_1) = \delta_2, f(\delta_2) = \delta_3, \ldots, f(\delta_k) = \delta_1. \tag{1.1}$$

A cycle is again an orbit, but consisting of recurrent points exclusively. Given a period order $k \geq 1$, then $\delta_{1\leq i\leq k} = f_k(\delta_{1\leq i\leq k})$ holds in general. If $k = 1$, we have a one-point-cycle, said the *fixed point* δ and the expression (1.1) boils down to:

$$\delta = f(\delta). \tag{1.2}$$

In the economy of dynamics over $\hat{\mathbb{C}}$, cycles may include finitely, infinitely or uncountably many points: their different topologies associate to different roles, whose mathematical details are unveiled by an appropriate local or global analysis. The global results over $\hat{\mathbb{C}}$, discovered during early XXth century, defined the two complementary sets of the '*basins* $\mathcal{B}$ *of attraction*' and of '*Julia set*' J. Each basin $\mathcal{B}$ is the maximal set of seeds whose forward orbits converge to the same neighborhood N of non-repelling fixed point. Most often, N includes a limit cycle of finitely many points; with regard to all local cases, *non-repelling fixed points do not necessarily match with the concept of limit cycle* in general. On the other hand, J could be totally disconnected and including infinitely many points, or a continuous line (Jordan or including double points); finally, it could be two-dimensional ($J \equiv \mathbb{C}_\infty$). J is the complement of the union of all basins, $\mathcal{F} \equiv \cup\mathcal{B}$, and it is also the boundary of $\mathcal{F}$: so $J \equiv \partial\mathcal{F}$ and $J \equiv \hat{\mathbb{C}}\backslash\mathcal{F}$. This union is also termed '*Fatou set*' in honor of Pierre Fatou (1878–1929), who co-pioneered these early global researches in the same times (1918–20) and independently from Gaston Julia (1893–1978), credited as the first official

discoverer[2] of the sets J in 1917–18.

Julia sets are well-known objects at all levels today, sparkling the imagination a wide range of people, from mathematicians to artists and to the curious. Their suggestive, very complicated fractal shapes were disclosed to human eyes through early computer experiments during late 1970s: machines accuracy, speed and screen resolutions became indispensable for unveiling the graphical details of their very complicate topologies, hardly reproducible via the handmade and rough drawings available to ancient mathematicians. For the eye, at least, not for the mind. The topological features were already clear to Fatou and Julia; although the Technology run is continuously reaching to finer and finer results and shorter computation times, this progress is not meant as a relevant leg along the whole road-map of holomorphic dynamics: speed and numerical accuracy are comfortable tools but they represent the 'brutal force' side of the deal and thus cannot turn mathematicians' eyes away from the development of methods deepening the analytical and geometrical laws determining our invariants. Machines are just means. The graphical methods may however rise to some nobility if developed along the 'intelligent' direction: algorithmically speaking, they are as efficient as the fine display is achieved by fitting the dynamical features of the given local invariants, not exploiting full machine performances. This especially holds true for local invariants, where specific methods are more often required. The textbooks [2, 6, 19] are good entry points to deepen these introductory concepts in mathematical terms.

After a first part on some introductory theory and culminating in the '*hedgehog*' definition, the second will go over most available techniques, shown to fail to display it adequately and finally we will blaze a trail in a new approach, with the support of pseudo-C++ code. We will begin to revisit a number of basic concepts in this field now; despite of their triviality, they will drive the reader along the further considerations which allowed to solve this practical problem.

2 Basic theory

2.1 The four cases

This is a sketch of the mathematics behind our local environment, where complex dynamics focus on the orbits behavior induced by the iterates $f_n(z)$ in the

[2](Related historical events are not fair.) Each basin relates to a same limit cycle. A fuller historiographic investigation will appear in [1].

neighborhoods of limit cycles for the function $f(z)$. For an easier approach, we will assume that invariants are just fixed points $\delta = f(\delta)$, but all next concepts extend to cycles of higher orders after minor modifications. Further observations will take on complex numbers in the Euler form: $z \equiv re^{2\pi i\theta}$. One initial difficulty is that they do not satisfy the Trichotomy law. But a classification necessarily wants them to be ordered under one real parameter. As previously mentioned, the linear part of $z_n = f_n(z)$ is an algebraic local invariant for any iterate of rank n. The question is then enlightened as one moves to the real tangent space by retrieving the modulus of the first derivative $\lambda \equiv |u| = |f'(\delta)|, u \in \mathbb{C}$ at the fixed δ. λ is a real value, being also the radius r in the Euler form. This achieves the sought order, regardless of the argument, as we find the 4 main classes of local dynamics around the fixed points:

1. *super-attracting*, when $|\lambda| = 0$;
2. *attracting*, when $0 < |\lambda| < 1$;
3. *indifferent* or *neutral*, when $|\lambda| = 1 = |e^{2\pi i\theta}|$;
4. *repelling*, when $|\lambda| > 0$.

2.2 Inclusion and exclusion

The terms in italics, for 1, 2 and 4, refer to the dynamical trend (towards or outgoing from the fixed point/periodic cycle); only the entry 3 escapes from this wording convention: dynamics are not uniquely determined here. This basic classification splits into two extremal cases: (super–)attracting and repelling dynamics, similar except for their opposite directions.

Standing in the middle, indifferent points play as a sort of conjunction between attraction and repulsion, in accordance to a dual (un–)relation: *inclusive* (the union of the opposites) when both attracting and repelling dynamics play around the fixed point. Or *exclusive* (the absence of opposites) when no attraction and repulsion applies. In global terms, one sees that (super–)attracting cycles are approached by forward iterates $f_n(z), n > 0$ and that Julia sets, including all repelling cycles, are accessible by backward iterates $f_n(z), n < 0$. Thus both successions of iterates run along a same road – the orbit – in one sense or in the other, from cycles of finite order to cycles of infinite order or viceversa. The indifferent type breaks up this trend, intimating to carefully revisit the 'limit' concept, for example, to accomplish its comprehension.

Whereas the modulus value was sufficient to feature the entries 1, 2 and 4, it could no longer apply to neutral points (see table 2.1), because the definition $|f(\delta)| = |\delta| = 1$ lacks of enough information. In fact $|u| = |f'(z)| = 1$ (or the radius r of u) is always set to 1, as well as its exponential part $|e^{2\pi i\theta}| = 1$, but the latter still includes one non-constant and real value. Thus it can be parameterized in the argument $0 \leq \theta < 1, \theta \in \mathbb{R}$. Analogously to the previous expedient, we move to an exponential space this time, determined by the real variable θ. First we differ 2 fundamental cases: when $\theta \in \mathbb{Q}$ (rationally indifferent δ, *parabolic* case) or $\theta \in \mathbb{R}\backslash\mathbb{Q}$ (irrationally indifferent δ, *elliptic* case). The former geometrically relates to one only invariant set, the Fatou-Leau flower (see def. at p. 81). While $\theta \in \mathbb{R}\backslash\mathbb{Q}$ branches out to a richer variety: the diagram 2.1 shows a sub-level opening to local invariant sets where θ enjoys different and extremely weak numerical properties, shunning the machine finite digits computation.

2.3 Analogies between linear models

The expansion of the derivative formula, together with the modulus, are helpful to start to understand the neighboring dynamics around the differentiated point: this familiar expression

$$\lim \left| \frac{f(z_0) - f(z_1)}{z_0 - z_1} \right| \equiv |\lambda|, \qquad z_1 \equiv z_0 + \Delta h, \quad \lim \Delta h = 0$$

may induce the reader to guess a straight classification of local dynamics through the geometrical description via one among three elementary motions in the plane: attraction ($0 \leq |\lambda| < 1$), dilation ($|\lambda| > 1$) and rotation ($|\lambda| = 1$), all represented by the linear map λz. This is not absolutely right nor completely wrong: in the dynamical terms of a whole family of iterates, one needs to prove whether the recursive process itself could enjoy the same possibility as it always does for one function $f(z)$ at once, i.e. whether $f_n(z)$ can locally turn into λz or not. In this reconsidered form, that initial guess was close to what pushed Schröder and, later, Koenigs to show that most holomorphic dynamics can be locally turned into λz. To this end, the crucial tool became the so-called *Schröder functional equation* (SFE), here in the general formula:

$$\psi[f(z)] = a[\psi(z)], \tag{2.1}$$

where $\psi(z)$ is an invertible map allowing $f(z)$ to be representable locally by $a(z)$. The goal of (2.2) is to set up an analogy between the local behavior of

iterates $f_n(z)$ around δ and an easier model. Without loss of generalization, let the origin be fixed for $f(z)$. Schröder and Koenigs succeeded to prove the analogy, strengthening the connection between SFE and holomorphic dynamics when they showed that $a(z)$ can be replaced with $\lambda \equiv f'(z)$; (2.1) turns as follows:

$$\psi[f(z)] = \lambda\psi(z). \tag{2.2}$$

Given a sufficiently close neighborhood D of δ, the chain rule for derivatives lets the left diagram below to be re-written in the right form extending to iterates, both commuting when the related SFEs hold:

$$\begin{array}{ccc} D & \to & f(D) \\ \psi\downarrow & & \psi\downarrow \\ \mathbb{C}_\infty & \stackrel{\lambda}{\to} & \mathbb{C}_\infty \end{array} \qquad\qquad \begin{array}{ccc} D & \to & f^n(D) \\ \psi\downarrow & & \psi\downarrow \\ \mathbb{C}_\infty & \stackrel{\lambda^n}{\longrightarrow} & \mathbb{C}_\infty \end{array}$$

If $\psi(z)$ can be represented by a convergent Taylor expansion, the SFE commutes and there exists a local change of coordinates where $f(0) = 0, f'(z) = \lambda$: the local behavior of orbits $f_n(z)$ can be then studied more simply through the linear map $\lambda^n z$. It is proven that SFE *always* commutes for (super–)attracting

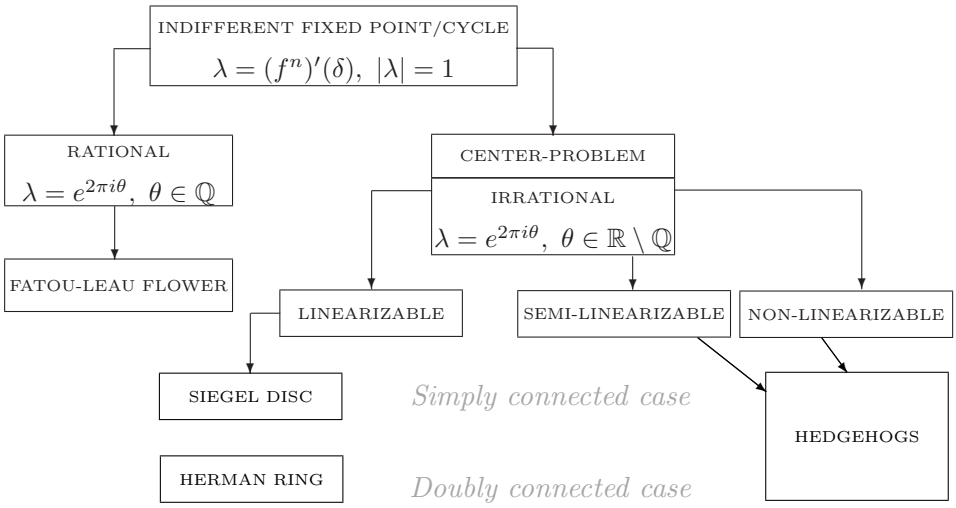

Table 2.1 : **Resuming the neutrality**. A diagram illustrating the classification of all dynamics for indifferent fixed points.

and repelling cases. If the local change of coordinates into λz applies, D is a **Böttcher** or a **Koenigs' domain**, when $|\lambda| = 0$ or $|\lambda| < 1$ respectively. For $|\lambda| > 1$, dynamics are locally repelling and regarded as the converse of the attracting ones; one merit, credited to Fatou and Julia[3], was to show that the

[3]According to their researches, one evinces the boundary role of repelling fixed points and cycles in the global dynamics all over the Riemann sphere. The former researchers did not score this goal, because they regarded repulsion like the converse of attraction.

role of repelling dynamics shall be completely reconsidered when the investigation extends to $\hat{\mathbb{C}}$, that is, acknowledged in the economy of the closure set of all repelling orbits (as resumed in diagram 2.2), according to the standard definition of **Julia set**, the common frontier for all basins $\mathcal{B}$ of convergence.

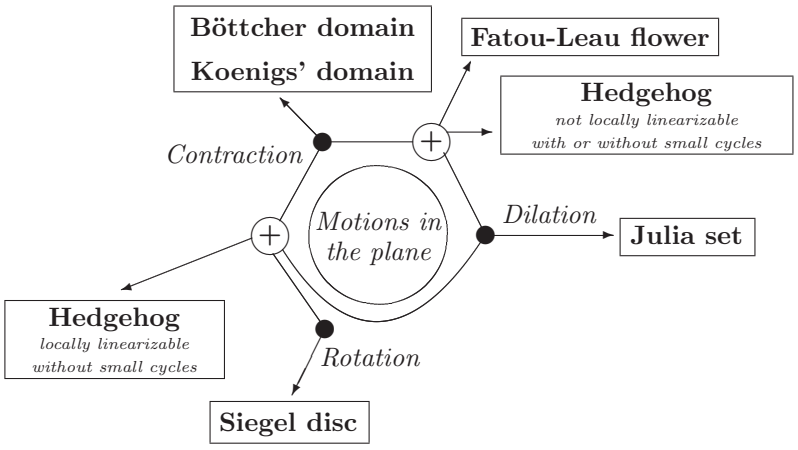

Table 2.2 : **Classification by motions**. Invariant sets for holomorphic dynamics in one complex variable seen via the three elementary motions in the plane.

As a counterpart to the previous easier cases, the discussion level is upset around neutral points (see list at p. 54): a much more delicate analysis, comparatively to the difficulties of the different situations for this case, is required. First, SFE re-writes as

$$\psi[f(z)] = e^{2\pi i\theta}\psi(z), \tag{2.3}$$

and for iterates $f_n(z)$, we have

$$\psi[f_n(z)] = e^{2\pi i\theta n}\psi(z), \tag{2.4}$$

conjugating (locally) to the family of complex rotations $e^{2\pi\theta in}z$: the problem was to determine whether (2.4) may hold for iterates of rational maps[4]. Resuming the core of studies from 1890s to 1940s, it was acknowledged that (2.4) never commutes for $\theta \in \mathbb{Q}$ whereas the numerical nature of $\theta \in \mathbb{R}\backslash\mathbb{Q}$ had to be elucidated for a definite response in this sense. After the first controversial results, Cremer (1920–30s) opened the road to a clearer perspective and Siegel finally (1942) closed such long period of doubt as he showed that the irrational θ shall satisfy this Diophantine condition[5] $\mathcal{D}_c$: given two numbers $r > 0, k \geq 2$,

$$|\theta - p/q| > r/q^k, \tag{2.5}$$

[4]The problem is trivial for polynomials.
[5]Formalized by Liouville decades before.

for every rational number p/q where $p, q \in \mathbb{N}$. Then iterates $f_n(z)$ are said to be *linearizable* into a complex rigid rotation or just 'linearizable' for short[6]; topologically speaking, there exists a neighborhood of δ which is conformally isomorphic to a rotatory disc by $f_n(z)$, the **Siegel disc**. When (2.5) holds, θ is *poorly approximated* by rational numbers; otherwise it is *goodly approximated* and no such linearization applies. It is clear that rational arguments (parabolic sub-case, $\theta \in \mathbb{Q}$) are not Diophantine and cannot satisfy (2.5): this also holds for a subclass of irrationals – the *Liouville numbers*. Now SFE is no longer useful and therefore one summarizes the previous concepts as follows:

• if SFE commutes around a (super–)attracting, or indifferent or a repelling fixed point, the local dynamics are classified by *just one* among these 3 elementary motions: *contraction*, *rotation*, or *repulsion* respectively;

• it also turns out that, when SFE fails to commute, local dynamics no longer consist of one elementary motion: there exist local vector fields, **Fatou-Leau flowers** or **Hedgehogs**, being compositions of more than one elementary motion. Thus one may state that the *SFE may shut the door to the local linearization of iterates at a fixed point.*

2.4 Hedgehogs, the next stop

Stepping in the second level of table 2.1 , let the holomorphic quadratic germ[7]

$$f(z) : e^{2\pi i\theta} z + z^2 + \dots \ . \tag{2.6}$$

Iterates $f_n(z)$ can be thus expressed in this form:

$$f_n(z) : e^{2\pi i\theta n} z + \mathcal{O}(z^k), \qquad n \geq 1, k \geq 2. \tag{2.7}$$

If compared to (2.3), the question boils down to the study of θ so that $\mathcal{O}(z^k)$ vanishes or not. It is straight-forward that, if $\mathcal{O}(z^k) = 0$, iterates do linearize and then show as $f_n(z) : e^{2\pi i\theta n} z$, i.e. rigid and aperiodic rotations (fig. 2.3 /A). Due to (neighboring) orbits feature, the point δ was termed *center* (of rotation) by Julia ([13], ch. IV) like Poincaré did for analogous points of ordinary differential equations:

[6]Let the map $f(z)$ be locally turned into λz, the definition indifferent multiplier yields that $\lambda = |e^{2\pi i\theta}| \equiv 1$; hence the linear map turns as $\lambda z \to e^{2\pi i\theta} z$, the mentioned rotation.

[7]Most results are subjected to this hypothesis. For germs of higher degrees, results are susceptible to modifications.

Definition 2.1 (Siegel Disc) *Let f be a non-linear complex function* (2.6) *and let δ be an irrationally indifferent fixed point, so that $|f'(\delta)| = e^{2\pi i\theta}$. If θ enjoys the diophantine condition* (2.5)*, the* SFE (2.3) *commutes and there exists a sufficiently close neighborhood $\mathcal{S}$ of δ, so that $\mathcal{S}$ is a simply connected component of the basin and analytically conjugated to an aperiodic rotation $e^{2\pi i\theta}$ of the unit disc $\mathbb{D}$.* ([19], p. 117)

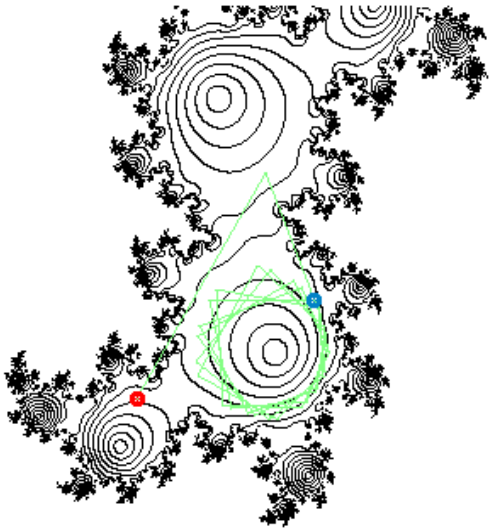

Figure 2.1 : **Singular dynamics**. Tracking down one orbit inside the basin with a Siegel disc $\mathcal{S}$. The red seed z_0 is iterated along the green orbit, until the final blue z_n falls into the disc. This figure was drawn by means of nested equipotential circles.

What happens if this condition is no longer met by $\theta \in \mathbb{R}\backslash\mathbb{Q}$? Recent Mathematics has been stressing that the concept of '*Natura non facit saltus*'[8] rules in dynamical systems. Related works ([10, 22, 29, 30], to quote a few) also showed that irrationals θ can gradually *drop off* the diophantine condition (2.5) and the Siegel disc $\mathcal{S}$ slowly turns into the hedgehog $\mathcal{H}$. For the above reason, we cannot expect drastic changes in the local geometry: in fact, the maximal $\mathcal{S}$ squeezes into a smaller disc, together with a complication of the neighboring orbits at $\partial\mathcal{S}$ while, at a semi-local level, the Julia set is wedging the surrounding basin $\mathcal{B}$ of attraction; when $\mathcal{S}$ is not maximal, $\mathcal{H}$ has a small linearization area. There are even irrational arguments θ so that $\mathcal{S}$ contracts finally to the fixed point δ: here $\mathcal{H}$ has no linearization area and δ is no more a center, but it is termed as a *Cremer point*[9].

[8] Ancient Roman phrasing by Linneus, alluding to Nature evolution by gradual and infinitesimal changes.

[9] In honor of Hubert Cremer (1897–1983) who first proved their existence when θ does not meet the Diophantine condition.

During 1920s and 30s, Cremer showed [11] that the set $\mathbb{R}\backslash\mathbb{Q}$ of all irrationals can be partitioned into two disjoint subsets $\mathcal{M},\mathcal{N}$:

• let $\mathcal{M}$ be the set of arguments θ so that $\mathcal{D}_c$ is enjoyed, then a maximal Siegel disc $\mathcal{S}$ exists; $\mathcal{M}$ is a full Lebesgue's measure set;

• let $\zeta \in \mathcal{N}$ be arguments whose value is a Liouville number. $\mathcal{N}$ is a null-measure set.

In the course of his proof on the existence of non-centers for rational maps ([11], p. 157), Cremer also showed that the existence of cycles of growing order n in the neighborhood of the non-linearizable indifferent δ and that they accumulate at δ as

$$\liminf_{n=1,2,...} \sqrt[s^n]{|\beta^n - 1|} = 0, \tag{2.8}$$

which holds for

$$\liminf_{n=1,2,...} |\beta^n - 1| = 0 \qquad \textit{and} \qquad \liminf_{n=1,2,...} \beta^n = 1, \beta = e^{2\pi i\theta}. \tag{2.9}$$

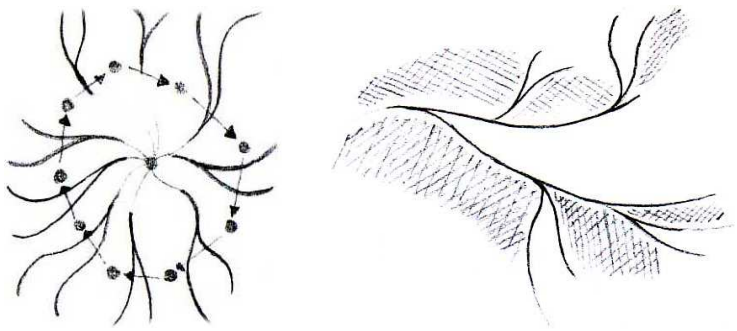

(A) (B)

Figure 2.2 : **Wedging the bounded basin (I)** Two hand-made drawings of the hedgehog entering the bounded basin (shaded region). The wedging white region is the basin of the point at infinity.

Because of the number of non–repelling cycles is finite (according to Koenigs' conjecture in 1883, proved later by Fatou and Julia) and according to the Julia set J nature (closure of repelling cycles), most periodic points of these cycles must be repelling[10] so that, roughly speaking, their accumulation shows that, as n grows, J keeps on wedging (see figs. 2.4 and 5.10) the bounded basin of attraction [10]: if $\limsup n = \infty$, then $\delta \in J$, otherwise the wedging action of J stops at a certain distance from δ for $\limsup n = K < +\infty$. (Again, the hedgehog $\mathcal{H}$ is the local invariant subset of the basin $\mathcal{B}$ and generated as the Julia set wedges $\mathcal{B}$.) The above limit may even tell that, algebraically, there

[10]Cremer never questioned on the nature of the accumulating cycles at δ throughout his works.

are cycles accumulating around δ and, topologically, that there are some neighborhoods of this fixed point and belonging to $\mathcal{B} \ni \delta$ or not, i.e. either to J or to another basin. This situation[11] also applies when 0 is reached in (2.8) so that $\delta \in J$: it occurs when α is rational or it is a Liouville number. Hence the poorly rational approximation — the diophantine condition for θ — implies a non-empty linearization area around δ, because cycles do not accumulate at it.

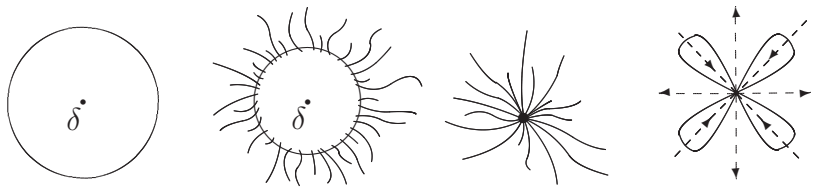

Figure 2.3 : **The ideal journey**. The local invariant sets for indifferent points, as watched during a journey where θ gradually loses its Diophantine condition: from the Siegel disc (A) to the Fatou-Leau flower (D). The filaments drawn in (B) and (C) mean to the Julia set wedging the basin while the disc is squeezing to the fixed point.

2.5 Journeying through the irrationals

The continuity may inspire a suggestive, ideal journey as we associate the topologies of different invariant sets from (A) to (D) to the numerical conditions met by θ as it goes from $\mathbb{R}\backslash\mathbb{Q}$ to $\mathbb{Q}$. The Siegel disc $\mathcal{S}$ squeezes (fig. 2.3 /B) until it disappears (fig. 2.3 /C); for both cases B and C, the invariant sets are 'hedgehogs' $\mathcal{H}$, when $\mathcal{S}$ is not maximal or has empty interior. Imagining this journey is possible in virtue of the strong unifying power offered by hedgehogs theory, which can link together apparently far dynamical configurations. The mathematical definition of the hedgehog $\mathcal{H}$ is [22]:

Definition 2.2 (Hedgehog) *Given a neighborhood U of an irrationally indifferent point δ, so that the holomorphic map f is univalent on U, the hedgehog $\mathcal{H}$ is an invariant compactum*[12]*, so that f is not linearizable or has linearization domain relatively compact in U.*

[11] This case is out of scope here. Anyway the Fatou-Leau flower dynamics are inductively helpful to watch how the basin to ∞ wedges the other basin, so that the Julia sets attaches to δ, assumed the germ $f(z) : e^{2\pi i\theta}z + z^n$, where $n \in \mathbb{N}^+, n \to \infty$ and $\theta \in \mathbb{Q}$.

[12] A compactum (plural, compacta) is a compact metric space.

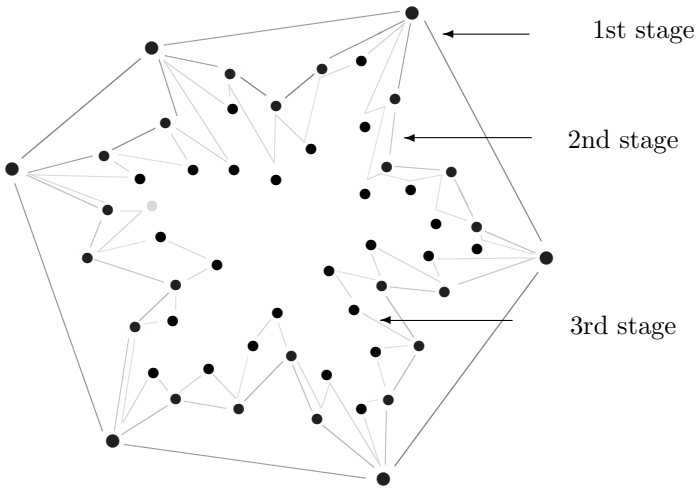

Figure 2.4 : **Hedgehogs generation.** An illustration of 3 steps (different shades of grey) of repelling cycles accumulation. The starred-shape, due to the cycles getting near δ, as well as wedging action of the Julia set J, are evident.

About (2.6), the current research is investigating on the semi–local dynamics around $\mathcal{H}$. Thanks to the results by Pérez-Marco in 1990 (resumed in [19], p. 123) one knows that $\mathcal{H}$ may show up in these different three characterizations:

1. hedgehogs $\mathcal{H}$ are locally linearizable and with no small cycles;
2. hedgehogs $\mathcal{H}$ are not locally linearizable and with small cycles;
3. hedgehogs $\mathcal{H}$ are not locally linearizable and without small cycles;

The '*small cycles*' property refers to the possible existence of infinitely many cyclic orbits in a sufficiently small neighborhood of the irrationally indifferent δ. It is said that 'δ *has the small cycle property*' or '*is approximated by small cycles*'. Other results on small cycles are included in [29, 30]. But this goes too far, beyond the scope of this introduction to hedgehogs, mostly intended to acknowledge the reader about the question on their digital visualization.

3 Entering the computer graphics

3.1 Features of ordinary methods

Most available methods for holomorphic dynamics perform a global action and are then devoted to the Julia set display. Often they do not focus[13] on the

[13]The approach by inverse maps achieves it, but it is not exportable to any maps because inverse ones cannot be always retrieved.

analytical properties of J. Both its location and shape come out from the human eye perception of the different colors distribution inside a close neighborhood of J. These methods do not draw J: they paint the Fatou set $\mathcal{F} \equiv \hat{\mathbb{C}} \backslash J$. So they are *not detective*, but *deductive*: focusing on the complement $\mathcal{F}$, they subtract it from $\hat{\mathbb{C}}$ so that J is deduced: $J \equiv \hat{\mathbb{C}} \backslash \mathcal{F}$.

3.2 Palette of colors

Suggested by experience, we address the following consideration to color Julia sets figures: the application of a palette sorted by (ascendent or descendent) shades[14] helps *to 'watch' the attracting and the repelling*[15] *direction of the family of iterates* between distant neighborhoods of the fixed point δ. The shading sequence points out to global dynamics, but fails to evince the local dynamics: the convergence/divergence rate slows down as orbits get closer to the indifferent δ and very close colors paint the neighboring domains, looking like the same to the human eye.

3.3 Convergence criteria

The fate of iterated orbits is tested at each $f_n(z) : z_n$, for preventing infinite looping. This is commonly achieved by a trapping disc $\mathcal{D}$ of given radius r, when $|z_n| < r$ is tested. This approach, aiming to understand when (in terms of the value of the iterative index i) orbits might escape $\mathcal{D}$, is commonly known as '*escape time*' algorithm. Some pseudo-code follows:

```
#include "complex.h" // this is a class handling complex numbers
                     // downloadable from author's site
complex z, next_z ;
complex c(0, -1);    // this is the complex parameter z = 0.0 - 1.0i

t = 50 ;             // top iteration index to prevent infinite looping
r = 2.0 ;            // the radius of the trapping disc

for( int i = 0; i < t ; i++ )
{
    next_z = z * z + c ;  // we assumed the quadratic iterator
    if ( abs( next_z ) > r ) break;

    z = next_z ;
}

take-some-color-value-from-the-iterative-index-or-from-the-point-z ;
```

[14]For example, of blue or gradients from green to violet.
[15]With regard to the nature of δ.

```
draw-z-on-the-screen ;
```

Another approach relies upon the distance between two successive iterates as test condition:

$$|f_i(z) - f_{i+1}(z)| < \epsilon, \qquad , \epsilon > 0 \tag{3.1}$$

It is a variant of escape time and defined the '*approximation*' method:

```
#include "complex.h" // this is a class handling complex numbers
                     // downloadable from author's site
complex z, next_z ;
complex c(0, -1);    // this is the complex parameter z = 0.0 - 1.0i

t = 50 ;             // top iteration index to prevent infinite looping
e = 0.00001 ;        // the distance ranging between 0 < e < 1

for( int i = 0; i < t ; i++ )
{
    next_z = (2*z*z*z+1)/(3*z*z) ;    // this is the transformed map
                                      // of z^3-1 by Newton's method

    if ( abs( next_z - z ) < e ) break;
    z = next_z ;
}

take-some-color-value-from-the-iterative-index-or-from-the-point-z ;
draw-z-on-the-screen ;
```

3.4 Obsolescence with local invariant sets

Our goal now is to discuss ways for bypassing or even lessening the two issues in sections 3.2 and 3.3. Anyway we remark that a new idea is most wanted and that as best as one can improve these methods, they will be however insufficient to obtain a fine drawing of what we seek. A first minor issue, discussed in section 3.2, refers to colors: gradients sequences are unfitting, so might a randomly generated palette help otherwise? In figures 3.5 , we iterated the neighborhoods around fixed points of different nature and painted them by the random palette. In figs. 3.5 /A and B, we consider the squaring map $f(z) : z^2$, with a super–attracting fixed point δ at 0; in (C), the Newton-Raphson method was applied to $f(z) : z^3 - 1$, having 3 attracting points on the unit circle $\partial\mathbb{D}$. One notices that both sequential and random palettes do work finely when iterated domains shrink to the attracting fixed point(s) step by step (analogously for the neighborhood of a repelling point). In figs. 3.6 and 3.7 , we tried to

(A) (B) (C)

Figure 3.5 : **Attempts of improvements**. The random palette coloring for attracting fixed points. More than the shading gradient approach, the attracting dynamics are evident here from the nested discs shrinking up to points.

draw the invariant sets (refer to fig. 2.3) arising around indifferent points δ, with emphasis to *colors sequence* and *numerical accuracy*.

For example, the iteration of the rationally indifferent germ $f(z) : z + z^4$ retrieves a Fatou–Leau's flower with 3 petals intersecting at the origin. Either applying random palettes or as infinitesimal values of ϵ are set into inequality (3.1), one cannot evince the local dynamics, but only the basins shape. And no benefits are drawn from the experiments with the irrationally indifferent points. In fig. 3.7 /A and B, the random palette and a very high number of iterates were respectively tested to work with a Siegel disc case (it should appear in the green basin). We tried to draw an hedgehog in (C, D). In particular, either (B) and (D) are displayed by another coloring method (said '*domain coloring*') which sets a one-to-one map between each complex point on the finite plane and the RGB cube, associating to one and only one color. Even if the iterative index i increases to very huge values, orbits cannot get very close to δ, so that no finer pictures can be obtained.

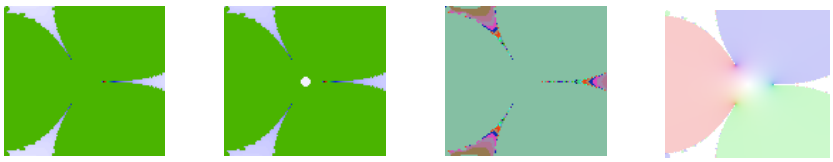

(A) (B) (C) (D)

Figure 3.6 : **Where are the flowered dynamics?** Different canonical methods applied to the Fatou–Leau flower and ...

Figures 3.6 and 3.7 attest that these methods, as well as any sort of variation, are unable to attain these local invariant sets as required, most important, in reasonable times. The main issue is that these methods feel a lot the convergence rate decrease at indifferent points.

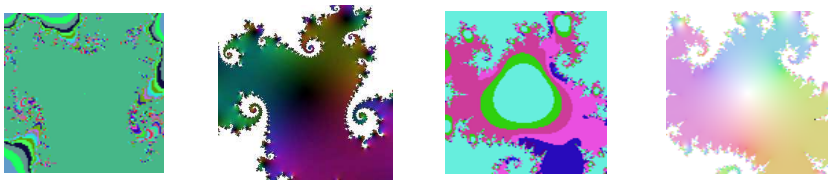

(A) (B) (C) (D)

Figure 3.7 : **Still veiled dynamics.** ... near a Siegel disc (A), (B) and an hedgehog (C), (D).

4 Off to 'composite dynamics'

The author was introduced to the problem of drawing hedgehogs on a computer by professor Pérez-Marco during an informal meeting at Perugia (Italy) on summer 2002 and fully reconsidered during Spring 2006. Milnor, in the appendix H of [19] (p. 244), also pointed out to the open question of retrieving fine pictures of local dynamics around non–linearizable indifferent points in reasonable times, with emphasis to the irrational kind: — '*For the fixed points of Cremer type, the situation is much worse. As far as I know, no useful computer picture of such a point has ever been produced!*'.

4.1 The core question

What should the drawing of a local invariant set focus on?

Without relying on a good response to this question, it might not make so much sense to continue. As remarked in table 2.2 at p. 57, holomorphic dynamics have different invariant sets. Globally speaking, Julia sets J are easy to display: one has just to tune the accuracy magnitude or set the top iterates index, according to the method applied as well as one fine palette.

In local terms, the neighboring dynamics at J points are collected under one concept: as orbits run across the basins $\mathcal{B}$ of attraction, their character, initially repelling near J, continuously changes while reaching the neighborhood of a non–repelling cycle (here, one fixed point δ). But some local invariant sets $\mathcal{I}_s$ around δ enjoy more or less complicated dynamics. The table 2.2 also offers an overview of invariant sets endowed with '*composite dynamics*', that is, involving more than one elementary motion. In geometrical terms, composite dynamics retrieve more than one information piece at one iterate, and thus they represent, even by a mere quantitatively viewpoint, an harder situation than those local dynamics involving one only elementary motion. One also remarks that the convergence speeds of neighboring orbits around the indifferent δ gets

slower as iterates get closer to δ; in the linear case of Siegel discs, convergence rate even stops to decrease as the modulus of iterates $|z_n| = |f_n(z)|$ arrests at one strictly positive value. These are symptomatic reasons of obsolescence, because the previous methods essentially work on chromatic representations for dynamics of attracting kind or, at the largest extent, of linear kind. Hence we conclude that the SFE shall be dropped off as well as the previous graphical methods: a new basis is required.

As we get back to non-linearizable local dynamics at $\mathcal{I}_s$, we shall consider that the previous mathematical discussion was helpful to have now some ideas of how dynamics are working around a Cremer point and thus of a glimmer of the sets topology around there somehow. After we caught an idea of the shape, we shall close the circle by rendering the true shape to such ideas. One then wants (1) to draw the boundary $\partial\mathcal{I}_s$ (graphically, the shape) and possibly (2) the motions therein (the orbits behavior). The accomplishment of (2) suggested us to focus on side considerations about the elementary psychology of Space, which is the perception of motion '*as lines in the principal directions of curvature, which may communicate surface shape better than lines in other directions*' ([12], p. 43). This is a common feature of the field of Non-Photorealistic Rendering (NPR), associated to the concept of '*perceptually efficient images*', meaning to the visual representation which emphasizes the important features and minimizes the superfluous details! This is a convenient concept to be regarded for our purposes and pushes to seek an analogously shaped geometrical model of the invariant set and being capable to evince both (1) and (2).

4.2 Obstructions (I) : no ticket for the ideal journey

Drawing local invariant sets around irrationally non-linearizable indifferent points mainly relates to the degeneration of the irrational argument $\theta \in \mathbb{R}\backslash\mathbb{Q}$ into a rational $\alpha \in \mathbb{Q}$, owing to *finite digits machine computation*. When θ is already rational, the question boils down to the convergence speed. We cannot want to attain the hedgehog on the wings of iterates exclusively, because we will approach to something differing from what we started looking for. Anyway we cannot quit to work with iterates at all! The strategy is then *to alleviate the error rounding off*. Throughout the following pages, in conclusion of some considerations on lacks and issues of several methods to display complex dynamics on a computer, we will show how this problem was algorithmically cracked for both the above numerical types.

Let the formula (2.7). One major issue is to check whether $\zeta = \theta^n$ could approximate irrationals poorly or not. One would like to distinguish the formal value θ with the input value α in practice, where $\alpha \approx \theta$: then $|\alpha - \theta| = \varepsilon > 0$. Analogously the iteration process may retrieve $|\alpha^n - \theta^n| = \rho > \varepsilon > 0$, with the growth of error magnitude. Then we cannot get contented of θ: could we make ρ tend to 0, if possible? More subtle issues may come up. In addition to numerical difficulties, even Topology grants no way out: Cremer's partition of irrational numbers shows that values $\theta \in \mathcal{N}$ cannot be picked up easily by a machine, in order to guarantee the chosen invariant set. The existence of hedgehogs $\mathcal{H}$ depends upon numerical conditions which are extremely weak for the machine decimals cut-off, that is, here dynamics feel a lot the approximation and their rendering cannot be pursued through methods relying on numerical computations exclusively. Again: *would it make sense to approximate a number $\alpha^n \in \mathbb{R}\backslash\mathbb{Q}$ via another irrational θ^n which possibly enjoys different numerical properties?* The value α^n might give rise to another local invariant set which differs, more or less evidently, from the one associated to θ^n. Cremer [11] observed that the null Lebesgue measure property does not imply that the set $\mathcal{N}$ is totally disconnected (pointwise); on the contrary, it may consist of disjoint intervals with positive, infinitesimal length $\varepsilon > 0$. *If machine approximation could work under at a certain magnitude $\varrho < \varepsilon$, we could afford to be more optimistic, in a way or another, of reaching a sufficiently sharp approximation for the original value α^n and of finding the related invariant set with adequate accuracy. At the same cost of long time computations anyway: whatever fast a computer might be then – times would not be decisively shortened because the whole process, in its intrinsic nature, lacks of efficiency* (see the end of introduction). Thus the numerical attack path is obstructed. At this point (!), Topology could be the only way out: having clear in mind that the digital representation would just offer an approximation of what non–linearizable local dynamics really are in the continuum, is there an alternative attack possibly approximating such kind of properties?

Running back into the approximation concept, we recall it refers to another entity β imitating, with a tolerable error, the original α. Hence we questioned on whether it is plausible to find out another, closer, value β and so that

$$|\alpha - \beta| < |\alpha - \theta|$$

holds? From the above, it seems that, if β, θ belong to a segment centered at α and whose width is $\leq \varepsilon$, then the approximation would make some sense. Otherwise, trying an approximation would throw us into a process generating

sequences of infinitely many values $\xi, \gamma, \ldots, \tau$ and this endless chain of nested inequalities

$$|\alpha - \beta| < |\alpha - \xi| < |\alpha - \gamma| < \cdots < |\alpha - \tau| < |\alpha - \theta|.$$

Could it be associated to infinitely many $\mathcal{P}$ between $\mathcal{P}_\alpha$ for the formal value α^n and $\mathcal{P}_\theta$ for working value θ^n? In fact, the chain nests as follows:

$$\mathcal{P}_\beta \subset \mathcal{P}_\xi \subset \mathcal{P}_\gamma \subset \ \ldots \ \subset \mathcal{P}_\tau \subset \mathcal{P}_\theta.$$

These speculations, together with the topological classification of hedgehogs at the end of section 2.5 – where small cycles may occur or not and which depend on such properties $\mathcal{P}$ of different nature, could give rise to the following questions:

Question 4.1 *Do we already know all numerical properties so that we can safely state to already know any hedgehog configuration? Can we find other numerical properties relating to new and unknown behavior of orbits inside hedgehogs? Thus, is their number finite? And, if so, how many are they?*

More generally one discusses on the possibility of moving from one property to another and, in our context of hedgehogs theory, the crucial question is:

Question 4.2 *Is there a way to move from one Liouville number to a Diophantine irrational value so that the ideal journey may come true ?*

These are questions we are not able to give a response; they arose during the inventing of our graphical approach.

4.3 Obstructions (II): practice really matters

Now with regard to the practical computations involved in the iteration process, we can find 3 obstructions to to hedgehogs, as drawn via ordinary methods:

1. *Statistical*: due to the $\mathcal{M}, \mathcal{N}$ sets distribution over the real interval $[0, 1]$, it much easier to pick up a value $\theta \in \mathcal{M}$ than one $\zeta \in \mathcal{N}$. And due to above approximation, this task gets harder than ever.

2. *Numerical*: numbers $\theta \in \mathcal{M}$ do not feel the approximation as much as $\zeta \in \mathcal{N}$; in fact, under iterates, Liouville numbers ζ tend to be turned into new values which are Diophantine irrationals; new resulting values cannot goodly approximate rational numbers and then one falls back into the Siegel disc case.

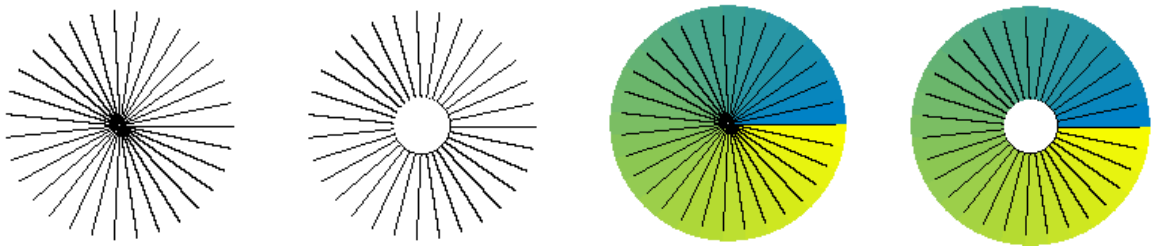

(A) (B) (C) (D)

Figure 4.8 : **I am the star**. The (holed) n^{th}-branched star in monochromatic and colored versions.

3. *Procedural*: Liouville's condition is fundamental to draw hedgehogs, but it is also weakly preserved under iteration. The orbits speed inside $\mathcal{H}$ slows down to the fixed δ. The remedy to get finer results is to let the iteration index n explode and we get back to obstructions 1 and 2.

No way out to overcome the two obstructions of approximation and computer usage. Hence, not having a valid solution at hand nor being successful to find it, the problem was left open until we occasionally came to it during March 2006, when we planned to find a strategy for *lessening the irrationality wipeout*. In the next section, the analysis on ordinary graphical methods for holomorphic dynamics will bring to their exclusion from the run for accurate displays of local invariant sets and, mostly, of hedgehogs.

4.4 Quality vs. quantity

Again, we also adduce that the methods described in section 3 are even *structurally weak* for our purposes: in fact, they have been developed (read, customized) for iterates of polynomial maps, in primis the quadratic $f(z) : z^2 + c$, where $z, c \in \mathbb{C}$ and c is a parameter. As we showed before, methods[16] might not work finely or at all when exported to dynamical systems being different from their original context. The ones we illustrated do work *quantitatively* and fail with dynamics claiming very sharp numerical accuracy; that is, the resulting geometry of invariant sets (both in local and global terms) is exclusively retrieved by the value of the last iterated point z_m, where m is the largest iterative index available to the machine architecture, at the higher costs of long computation times.

[16]This also happened to for quaternionic Julia sets, where the author revisited the analogous escape time method so to display even those Julia sets which are not closed and bounded curves, but extend to point at infinity [24, 25] (one example is the Newton-Raphson method applied to the cubic $h^3 - 1 = 0, h \in \mathbb{H}$, where $\mathbb{H}$ is the quaternion space).

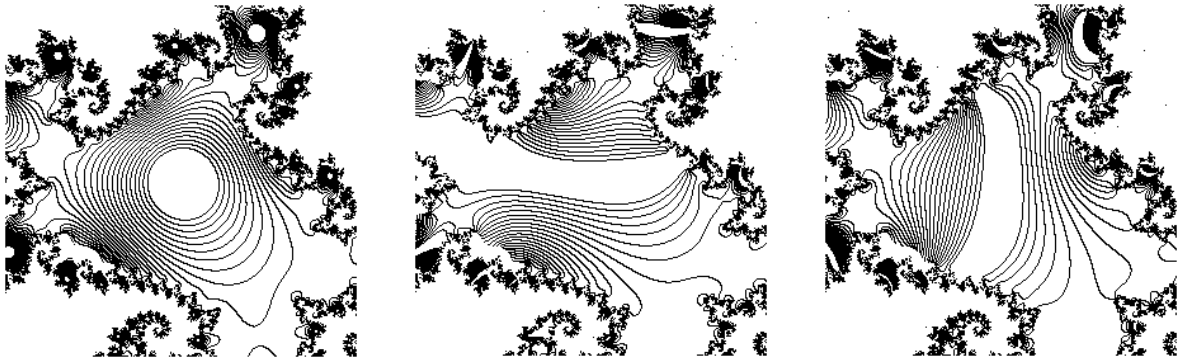

(A) (B) (C)

Figure 4.9 : **Trying some linear equipotential models**. These are equipotential renderings based upon the linear models of concentric disks (A), vertical (B) and horizontal bands (C). All fail to evince the hedgehog shape.

Saving time and resources, improving speed and accuracy are goals of Automatics: even at the cost of indirect attack (a sort of cheat, then!), we found a way out as we opted to not approach the neighborhoods, but to '*be-already-there-and-work-with-orbits*'. This new direction cannot avoid the method customization: we adopted an half-way strategy which, besides the inevitable finite digits computation, teams up with a *qualitative* attack by *the imitation of a model with pre-defined shape*. More explicitly, all this came after the conclusions in section 2.3, where the failure of SFE for Fatou-Leau flowers and hedgehogs implied that such dynamics *cannot be adequately described by linear models based upon regular curves, such as concentric circles (isomorphic under rotations) or straight-lines bands* (see figs. 4.9). So we liked to use a non–regular and (mostly) *topologically equivalent non–linear model*. Namely it is the (holed) n^{th}*-branched star*, whose versions have been depicted in table 4.8 . It is extremely important to remark that the following results use the quadratic germ (2.6) exclusively: the theory on irrationally fixed points came to the today robust status for this degree only by now; an attack to the iterates of such holomorphic germs of higher degrees is documented in [31].

5 Re-elaborating the equipotentials

Related graphical examples can be found inside [20] by Needham and, for holomorphic dynamics, in [19] by Milnor – although they weakly already appeared in older publications [21, 23]. In particular, [19] (p. 123) was rather inspiring to try enhancing graphics as it focused on an imitation graphical model based upon equipotentials; it also includes the continuous fraction formula of

an irrational argument θ:

$$\frac{1}{3+\frac{1}{10+\frac{1}{20000+\ldots}}}, \tag{5.1}$$

yielding an hedgehog with small, non-empty, linearization domain, together with an (intuitive) figure of it.

5.1 The holed n-th branched star model

The approach roots to one method often applied to dynamical systems, in general, and in complex analysis too. It is known as '*equipotential curve*'. The pseudo–code below was reported to aid the explanation rather than to offer an implementation (in order to lessen the translation to another favorite language): it consists of a main routine taking on the input finite subregion of $\mathbb{C}$ as a grid of seed points z_0; then the holed star model checks whether the dynamics of the orbit z_n should be drawn.

```
#include "complex.h"  // this is a class handling complex numbers
                      // downloadable from author's site

complex fxd_pt ;      // we assume to already know the hedgehog
fxd_pt.real = 0.0;    // is around an indifferent fixed point
fxd_pt.imag = 0.0 ;   // at the origin

double val = 0, tmp_val = 0 ;   // these are containers which will
                                // be later stored and compared

BOOL bInitFlag = FALSE ;        // this boolean flag is used
                                // to check the two previous
                                // container of [double] type

// the four coordinates (top/x1, left/y1),(right/x2,bottom/y2)
// of the screen port are stored in these containers;

int top = 0, bottom = 320, left = 0, right = 200 ;

complex z ;

for ( x = left + 1; x < right ; x++ )
{
    for ( y = top + 1; y < bottom ; y++ )
    {
        // there are different ways to perform this conversion.
        // we opted to this backward map from screen coordinates
        // to the complex plane, assuring that each screen point
        // is associated to one complex z.

        rescale-the-pair ( x, y ) to-the-pair ( z.real, z.imag );
        ////////////////////////////////////////////////////////////
```

```
            // then iterate the function for the required number of steps
            // with no test conditions. Refer to the previous code.
            // Stop the loop through the iterative top index limiter.

            // We chose to not show the related code for the iterated
            // function because more complicate explanations would be needed.
            // Make sure you are working with a suitable map retrieving
            // an hedgehog. We suggest you to use the one below: an
            // holomorphic quadratic and indifferent germ whose argument
            // theta is given by the continuous fraction reported further.

            // We can say we coded a complex parser
            // to input any function even in the form; sorry
            // but the latex syntax is the best we can use to
            // arrange one example:
            // f(z) : e^(2\pi i\theta)z+z^2

            complex output_z = iterate-the-function f(z) ;

            // NOTE : if you input the identity map, you'll see
            // the holed branched star.

            BOOL bDraw = Holed_Star( output_z, fxd_pt, double& val,
                                     double& tmp_val, BOOL& bInitFlag ) ;

            if ( bInitFlag )
            {
                if ( val != tmp_val )
                {
                    if ( bDraw ) pDC->SetPixel( x, y, 0 );
                    val = tmp_val ;
                }
            }
            else bInitFlag = TRUE ;
        }
    }
```

The two nested `for` cycles perform a *raster*[17] *scan* of the screen port by rows (`y`) and columns (`x`); each point associates to a pair of positive integer coordinates which is turned into a couple of real and imaginary values, so to finally obtain the complex point `z`=`x`+i`y`. The following are code details around the function `Holed_Star`, drawing the hedgehogs/holed star by equipotentials: below we show how to render a monochromatic hedgehog (refer to table 4.8 /A and B); the colored version requires one more function handling colors, but we chose to not include here for keeping a easier approach to the code.

```
BOOL Holed_Star( complex z, complex fxd_pt, double& val,
                 double& tmp_val, BOOL& bInitFlag )
```

[17]This is a technical term in computer science to indicate that an image is regarded as a mesh of points distributed along rows and columns; each point is associated to a triplet of values. The first two values are the unique pair of coordinates which define the location in the mesh. The third value is an index referring to color, usually defined in the RGB additive model.

```
{
    #include "complex.h" // this is a class handling complex numbers
                         // downloadable from author's site

    #define PI 3.14159265358979323846  // we need PI to be the
                                       // sharpest as possible

    complex tmp_z = z ;          // we need another container for
                                 // storing a temporary value later

    double branches_number = 12 ;      // this explains itself !
    double offset = 0.5 ;              // it is the radius of the
                                       // hole in the star: when
                                       // set to 0, the disc is empty

    double existence_interval = 2.0 * PI ;   // the full range of values for
                                             // computing all branches location
                                             // in radial terms

    double potential_rate = existence_interval / branches_number ;

    tmp_z -= fxd_pt ;            // all points are translated so that
                                 // the fixed point is mapped to the
                                 // origin and the computations get easier

    double v = tmp_z.angle();
    double out_level = ( f.euclidean_dist( z ) <= offset ) ? -1 : v / potential_rate ;

    int ol = (int)out_level ;       // this integer is used for the output
                                    // level and possibly to color the point

    if ( !bInitFlag ) val = ol ;    // if this flag is not set, then it is
                                    // the first value to be stored.
    else tmp_val = ol ;             // Otherwise, it does not. Refer to
                                    // the main function before

    if( ol < 0 || ol > branches_number )     // check for values ranging
                return FALSE ;               // out of the interval

    return TRUE ;
}
```

We have now a bunch of code to be cyclically applied for scanning the input complex bounded region $\mathcal{R} \subset \mathbb{C}$, so that `Holed_Star` classifies the n–fold image region $f_n(\mathcal{R})$ via the star model.

5.2 Unveiling the code

Here we explain the computations performed in the main parts of the code of section 5.1. First we focus on:

(A) (B) (C)

Figure 5.10 : **Wedging the bounded basin (II)**. Three close-ups of the wedging action along the hedgehog $\mathcal{H}$ generation as the iterates of (2.6) with θ (5.1) are rendered through the holed star model. The top iteration index was (just!) set at (A) 150, (B) 300 and (C) 1000 respectively. White disks are preimages of the star hole; colours change depending on the iteration values attained by the forward images, in respect of their original distribution (refer to fig. 4.8).

```
double out_level = ( f.euclidean_dist( z ) <= offset ) ? -1 :
v/potential_rate ;
```

if the distance of point `z`, resulting from the iteration process, to the fixed point `f` is larger than a preset value `offset`, then the ratio `v/potential_rate` is computed in order to know whether the iterated point shall be painted black or not. Otherwise the negative value -1 is used as a flag indicating that the point shall not be tested again. The container `offset` stores the radius value for the hole in the star model. The value `v` is the argument of the last image `z` in the current orbit and helping to have that point location in relation to the branches. One also notices that

```
double potential_rate = existence_interval / branches_number ;
```

when applied to the first line of code, `v / potential_rate` turns into

$$\texttt{index} = \frac{\texttt{v} \cdot \texttt{branches\_number}}{\texttt{existence\_interval}} = \frac{\texttt{v}}{\texttt{existence\_interval}} \cdot \texttt{branches\_number}.$$

The ratio on the right is normalized to the unit interval $[0, 1]$; when it is multiplied by `branches_number`, one finds that:

$$0 < \texttt{index} < \texttt{branches\_number}.$$

So `index` ranges in the interval of given number of branches. If decimal values are retrieved, they are rounded off to the lower integer: in fact decimals do not make sense in terms of branches index. For example, given 31 branches for the holed star of table 5.13 , we expect the `index` ranges between $[0, 30]$. The right product with `branches_number` yields the branch index for the last computation of the n–iterated point.

5.3 Trespassing the equipotentials

Thus it is reasonable to wonder now: *given a white background, how come are black lines painted exclusively?* Moreover (since black pixels refer to the only points to draw) *why are others not painted?* Just because one method generally relies upon the condition of *trespassing* equipotentials to draw screen points.

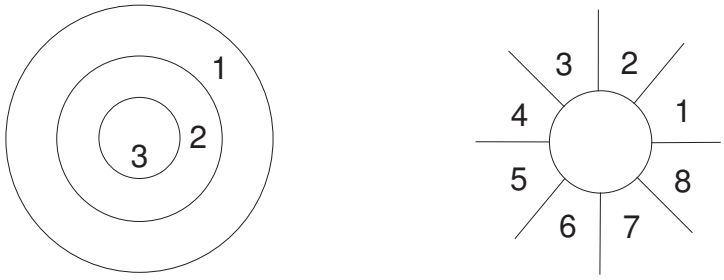

Figure 5.11 : **Indexes for equipotentials**. Numbers represent the equipotential levels distribution in the two models: nested circles and holed star. When indexes change, the final point belongs to one indexed region instead of another (the two regions are adjacent because of continuity), and thus the equipotential curve between is trespassed.

Our computational model looks at the curves locus playing the qualitative role and it is often described by one formula. (For example $|z-\zeta| = R$ describes a circle centered at ζ or we have an open disc if '=' is replaced with '<'.) For meeting the machine efficiency, we need to deal with quality, but in terms of quantity: so each curve associates to one only index value. When we point out to one curve or to one branch in the star model, we want its index. The expression '*trespassing the equipotentials*' means that, given the final index value associating to the last iterated point of an orbit, the analogous point of the next computed orbit, has *changed*. For a set of points whose orbits retrieve the same index, only the first one shall be drawn; again, if the indexes of two consecutive points are different, the equipotential curve was trespassed and the second point is drawn then. Algorithmically speaking, one stores the last index and, if it equals the previously stored value, no equipotential is trespassed; otherwise, the related point is painted black. Implications are straight-forward:

Different indexes $\rightarrow$ *Different equipotential* $\rightarrow$ *Trespass* $\rightarrow$ *Paint the point.*

For example, if we associate each screen point to the resulting branch index, we find out a chain of indexes which then indicates how pixels and the entire screen row are processed along the raster process from left to right:

1-1-1-2-2-2-2-2-2-3-3-3-3-4-4-4-4-2-2-2-5-5-5-5-3-3-3-3-3

The underlined indexes are those *making the difference* and each one of them arrests the previous sub-sequence of same values. The point, relating to the underlined index, is painted black in our monochromatic version (for colors, we associate the index value to the color index in the palette). Technically this can be easily understood by handling the boolean flag `bInitFlag` of the main routine at section 5.1. The reader would take care that, as the `bInitFlag` is set, comparison values are stored in the two containers `val` and `tmp_val`, shown below in the code explaining how the trespass is handled:

```
BOOL bDraw = Holed_Star( output_z, fxd_pt, double& val, double&
tmp_val, BOOL& bInitFlag ) ;

if ( bInitFlag )
{
    if ( val != tmp_val )
    {
        if ( bDraw ) pDC->SetPixel( x, y , 0 );

        val = tmp_val ;
    }
}
else bInitFlag = TRUE ;
```

It is clear that the old equipotential is trespassed and the point is painted black (the RGB triplet is set to 0) only when

```
if ( val != tmp_val )
```

So we 'jump'[18] to the adjacent equipotential level. And the new value `val = tmp_val` is taken on for further comparisons.

5.4 Stars and equivalent classes

With regard of their fate (see section 5.5), the holed star model classifies orbits z_n into equivalence classes

$$\mathcal{E}_1, \mathcal{E}_2, \ldots, \mathcal{E}_k,$$

where k is the number of the branches. For any bounded top index, the iterate z_n has necessarily one argument $0 \leq \theta < 2\pi$, thus every orbit inside the bounded basin $\mathcal{B}_\delta$ must necessarily belong to one such equivalence class: this is straightforward but suffices to state that $\bigcup_{n=1}^{k} \mathcal{E}_n$, can describe the whole bounded basin.

[18]Iterations give rise to discrete systems, then a jump is the movement from one equipotential level to another adjacent (previous or next).

Orbits of the basin $\mathcal{B}_\infty$ cannot reach to the holed star thus, empirically speaking (since every orbits belongs to the class defined by the branch it lands on), they do not belong to any class $\mathcal{E}_k$. Again, the holed star model maps $\mathcal{B}_\delta$ to the union of the regions between the branches. The equivalence classes allow to reconstruct the basins distribution in the same fashion as of the star model: so one also understands why it also works finely with the Fatou-Leau flower, a similarly shaped vector field, where one basin wedges the other.

The branches of the star model elongate from the outer region up to the disc, or to the center point if the hole has zero area: this is not merely obvious and plays relevantly during orbits classification. In a similar fashion but when applied to iterates, the imitation of the branches distribution allows to track down the wedging action of $\mathcal{B}_\infty$ up the boundary of the hole or, again, to the center of the star when the hole is empty: even here, consequentially, the wedging action by $\mathcal{B}_\infty$ to $\mathcal{B}_\delta$ helps to understand the hedgehog shape (*this is the reason why one needs to know the radius value.*) Along a different path than in section 5.5, we came to the same great benefit: the graphical imitation, *up to the hole boundary*, performed by the holed star with regard to hedgehogs and, as we will see further, for Fatou-Leau's flowers too, since they enjoy a similar, less complicate, starred topology.

5.5 The pro(s) and con(s)

Benefits: according to our approach of 'being-already-there-and-work' (p. 71), orbits $f^n(z) : z_n$, which finally reach to a same equipotential level $\mathcal{R}$ (the bounded region radially distributed around δ), are collected under a same color. From the early works by Cherry [10] and the later production by Pérez-Marco [22], hedgehogs dynamics can be simply resumed as follows ([10], p. 33):

> *"... as it progressively deformed through starfish shapes* [...] *consisting of an infinity or 'rays' emanating from O* [the origin]*; each such 'ray' is a connected closed set, and 'most' of them are arbitrarily short. A z_0 on any of these rays gives a chain (z_n), each of whose points lies on another of them ..."*

From figs. 5.10 , both the star contour drawing[19] and the color painting help to evince the shape of $\mathcal{H}$ by a comparatively little iterative index, whereas other methods – even if pushed to the top machine performances – would have never

[19] In equipotential terms, it is the same as drawing the contour of the star.

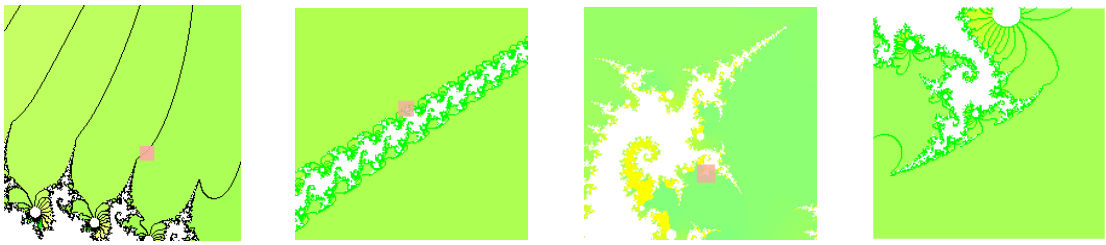

(A) (B) (C) (D)

Figure 5.12 : **Wedging the bounded basin (III)** In (A), we moved to the basin boundary $\partial\mathcal{B}$ for tracking down the hedgehog wedging action since the beginning. The filaments, where hedgehog subsets are of infinitesimal size, have been chosen for taking the successive close-ups (red squared regions). In (A) we started from $\partial\mathcal{B}$ and applied a small number of iterates (just 100); the elongating lines to the top of the figure are a side effect of the holed star equipotential, showing the hedgehog wedging direction. From (B) to (D), a bit larger iterative index (circa 200) grants to see that the degree of complication grows with the appeareance of several infinitesimally small fjords emanating from the longest arm which keeps on running towards the linearization domain (empty or not).

reached there. Good pictures on the wedging action can be granted because of *the holed star resembles the hedgehog topology*, with no need of inputting very huge index values for obtaining almost the same results as previous standard methods may do, because of the very slow speed of neighboring orbits z_n around δ. So this approach completely fills the lack of the previously discussed methods. All in all, the star model benefits are two-fold: while the regions imitate as best as possible such dynamics inside the bounded basin, the branch lines are screening the shape of the basin $\mathcal{B}_\infty$ to ∞. Since the latter and the bounded basin are complementary sets, in terms of converging orbits, tracking down their shapes equals to know the hedgehog topology. In fact, we can understand where fjords will tend to (figs. 5.12). Equipotential models, endowing with different graphical styles, may be thought as sort of interpreters, where the fittest one 'speaks in the same terms' as the local dynamics at a fixed point of $f(z)$.

Lacks: more than any other equipotential model, the holed star does not grant an 'intelligent approach', that is, able to fit the topological characters of any local invariant set, given the input function $f(z)$. Equipotential curves just play as a sort of elastic sheet stretched by the action of $f(z)$ and they are used then to look at the local dynamics via distributed lines: one then understands that the knowledge of given local set properties is required for the most fitting choice of the equipotential model among a bunch of them featuring different distributions (horizontal or vertical straight-lines, concentric discs, stars): in fact each model works differently on a same case and thus may be more or less reliable. The hedgehog and the holed star model even enjoy this empirical rule, so the fine tunings for the star may ensure the most resembling results.

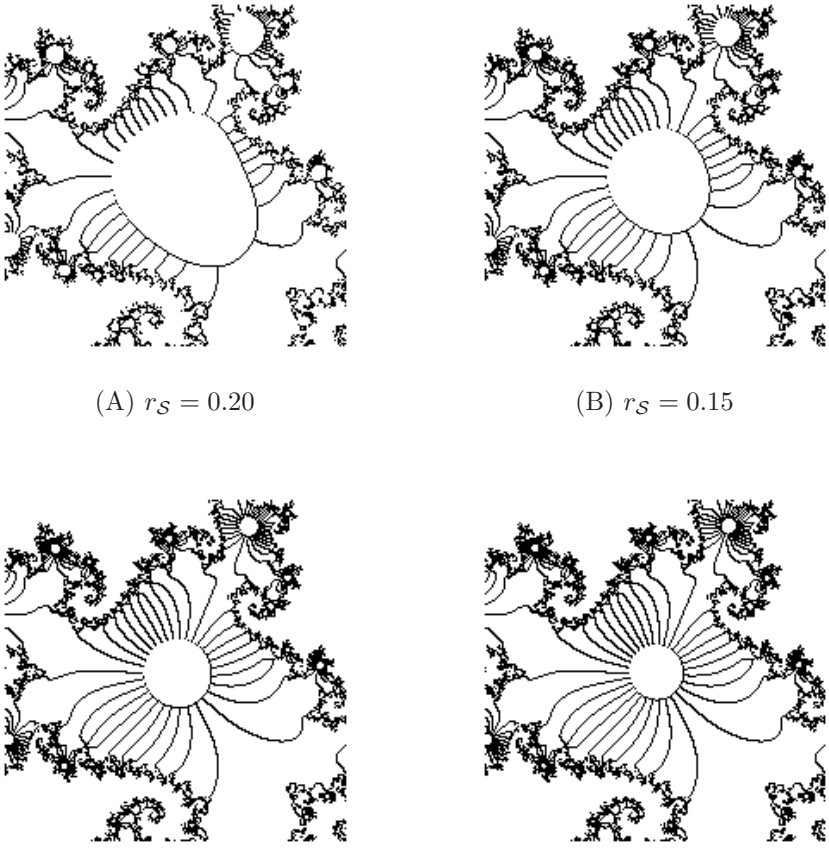

(A) $r_{\mathcal{S}} = 0.20$ (B) $r_{\mathcal{S}} = 0.15$

(C) $r_{\mathcal{S}} = 0.10$ (D) $r_{\mathcal{S}} = 0.09$

Figure 5.13 : **The radius test**. Tuning the radius $r_{\mathcal{S}}$ of the Siegel compactum.

The holed star enjoys a less 'ready–to–go' approach than concentric circles or straight lines equipotentials, because both the hole radius and the branches amount shall be finely tuned.

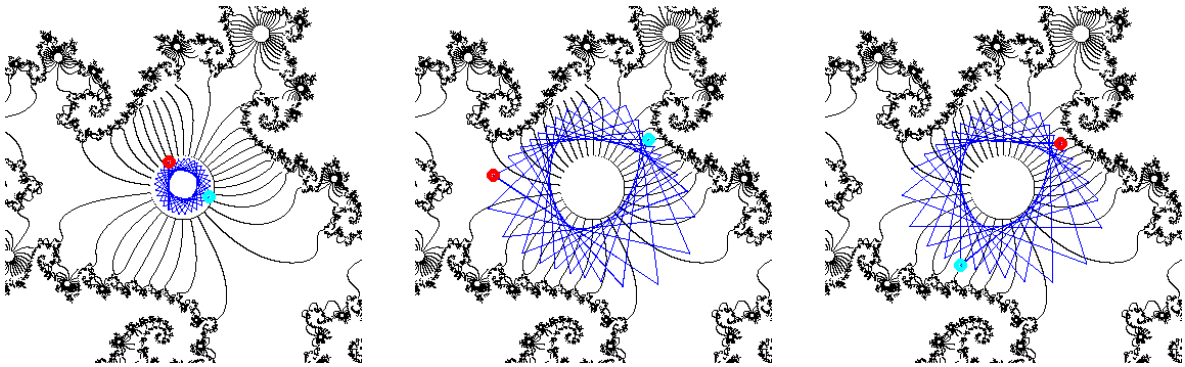

(A) (B) (C)

Figure 5.14 : **Neighboring dynamics**. Figure (A) shows the rotatory motion of iterates in the Siegel compactum, while outer orbits are shown in (B) and (C). According to the caption of figs. 5.12 , the filaments in this full view show how the hedgehog is wedging the whole basin of attraction.

5.6 Tuning the disc radius

The figures 5.13 show the results corresponding to different tunes of the maximal disc/hole radius $r_{\mathcal{S}}$. Fine tunes are then required: for large values, the hole boundary is rather deformed, whereas smaller radii retrieve discs which may not evince the true extension of the Siegel compactum. The problem of determining a sharp estimation of the Siegel disc radius was mathematically discussed and cracked by the author: it represents one application of a wider theory which will be the object of a later work [26]. In figure 5.13 /D, we set the hole radius to the value resulting from such computation. The joint application of computer aided graphics and Mathematics will be finally helpful to obtain a fine version of hedgehogs pictures.

5.7 Displaying the Fatou-Leau flowers

Since the holed star model was acknowledged to work finely for the hedgehog — one might like to extend it to Fatou-Leau's flowers as we did in table 5.15 , since both invariant sets are resembling as well as flowers can be regarded like stars with empty hole (radius is 0).

Definition 5.1 ***Fatou-Leau flower.*** *If $\hat{z}$ is a fixed point of multiplicity $n+1 \geq 2$, then there exist attracting petals $\mathcal{P}_1, \mathcal{P}_2, \ldots, \mathcal{P}_n$ for the n attracting directions*

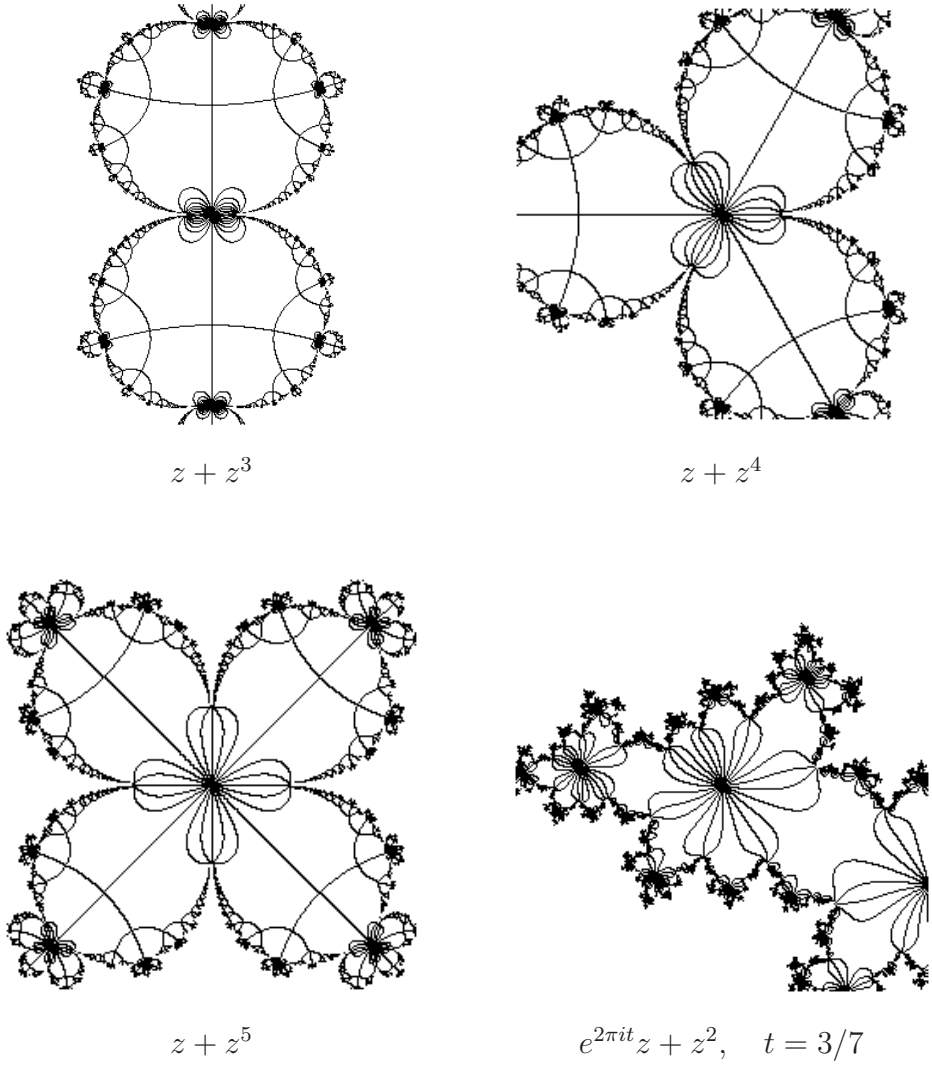

Figure 5.15 : **A bunch of flowers.** The application of the holed star to different configurations of the Fatou-Leau flower.

at $\hat{z}$, a repelling petals $\mathcal{P}'_1, \mathcal{P}'_2, \ldots, \mathcal{P}'_n$ for the n repelling directions, so that the union of these $2n$ petals, together with $\hat{z}$ itself, forms a neighborhood N_0 of $\hat{z}$. ([19], p. 105)

One first notices that straight lines meet at the origin and they lie at the attracting directions, whereas the divergent ones are deformed into petals-shaped curves. Like for any indifferent point, the convergence speed rate slows down in the flower neighborhoods; even here, the holed star model helps to go all the way down to δ and save long time computations. It is also useful to remark that here straight segments to the origin are drawn by orbits inside the converging petals. The application to these flowered invariant sets plays as another evidence attesting the benefits of such a qualitative approach; again the star parameters need to be tuned appropriately, although it is much easier

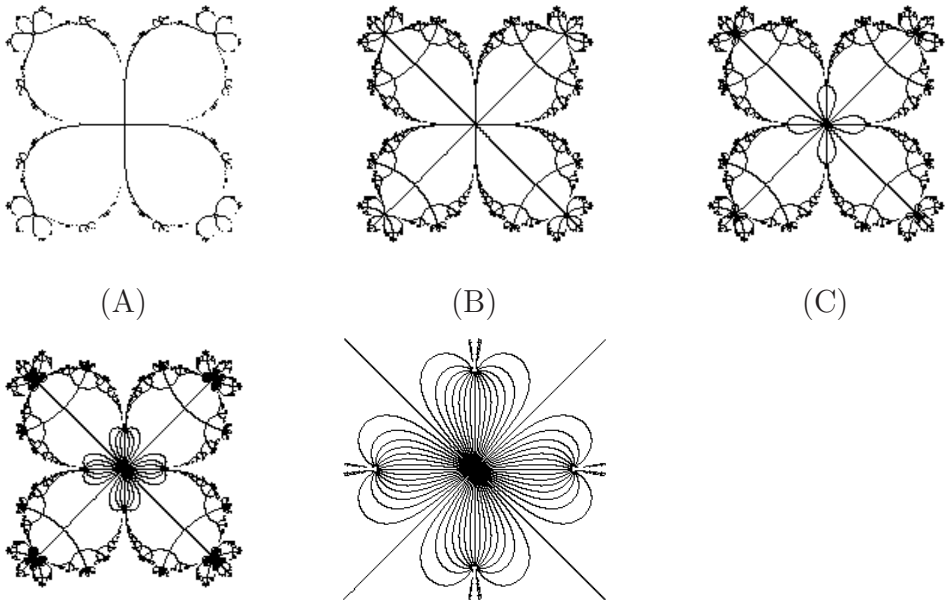

(A) (B) (C)

(D) (E)

Table 5.3 : **Tuning the number of branches**. The iteration of $f(z) : z + z^5$ yields a flower with 4 petals. A better performance is guaranteed when star branches are adjacent to all the 4 converging and the 4 attracting directions; thus 4 is the smallest number to obtain only the attracting directions (A). Multiples of 4 are suggested to have finer pictures of the dynamics inside the petals as in figures (A), (B), (C), (D), (E) where 4, 8, 16, 32 and 64 branches have been respectively set.

here: in fact the radius hole is always 0 and the branches number can be easily found mathematically. For more correct pictures, one shall be sure to set them adjacently to the alternating (convergent and divergent) directions.

6 Acknowledgements

The author thanks the editorial board of the journal "Electronic Journal of Differential Equations and Control Processes" for accepting this article for publication.

7 Conclusions

In author's opinion, well-drawn figures of local invariant sets necessarily want customized approaches: empirically, equipotentials seem the best performing today, susceptible to optimizations coming from the application of topologically equivalent models. A general method working for any local invariant set, independently from the input map, thus could be a utopia. Keeping on being

open-minded to any possibilities offered by Science, anyway one optimistically would like to add the words '*up to now !*'

Alessandro Rosa

zandor_zz@yahoo.it

References

[1] Alexander D.S., Iavernaro F., Rosa A., *Early days in complex dynamics*, in preparation.

[2] Beardon A.F., *Iteration of rational functions*, Springer & Verlag, 1991.

[3] Binder I., Braverman M., Yampolsky M., *On computational complexity of Siegel Julia sets*, Commun. Math. Phys, preprint.

[4] Buff X., Chéritat A., *On the size of quadratic Siegel disks. Part I*, Prepublication du Laboratoire É. Picard, n. 267, Toulouse, France, 2003.

[5] Buff X., Chéritat A., *Upper bound for the size of quadratic Siegel disks*, Inventiones Mathematicæ, 156, 1, 2004, pp. 1–24.

[6] Carleson L., Gamelin T.W., *Complex Dynamics*, Springer-Verlag, New York, 1993.

[7] Cayley, A. *Applications of the Newton–Fourier Method to an Imaginary Root of an Equation*, Quar. Journ. Pure and Appl. Math., 16, 1879, pp. 179–185.

[8] Cayley, A. *The Newton–Fourier Imaginary Problem*, Amer. Journ. of Math., 2, 1879, 97.

[9] Cayley, A. *On the Newton–Fourier Imaginary Problem*, Proc. Camb. Phil. Soc., 3, 1880, 231–232.

[10] Cherry T.M., *A singular case of iteration of analytic functions: a contribution to the small divisors problem*, Non-linear problems of Engineering, Academic Press, New York, 1964, pp. 29–50.

[11] Cremer H., *Zum Zentrumproblem*, Math. Annalen, 98, 1927, pp. 151–163.

[12] Girshick A., Interrante V., Haker S., Lemoine T., *Line direction matters: an argument for the use of principal directions in 3D line drawings*, Non-Photorealistic Animation and Rendering, Proceedings of the 1st international symposium on Non-photorealistic animation and rendering, Annecy, France, 2000, pp. 43–52.

[13] Julia G., *Mémoire sur l' itération des fonctions rationnelles*, Journ. Math. Pur. Appl., (8), 1, 1918, pp. 47–245.

[14] Koenigs G., *Recherches sur les substitutions uniformes*, Bull. Soc. Math. Astr., Series 2, 7, Part I, 1883, pp. 340–357.

[19]This article was submitted on December 2006 and approved for publication on January 1st 2007. The author site: http://www.malilla.supereva.it

[15] Koenigs G., *Recherches sur les intégrales de certaines équations fonctionnelles*, Ann. Sc. Éc. Norm. Sup., Séries 3, 1, 1884, pp. 1–41.

[16] Koenigs G., *Nouvelles recherches sur les équations fonctionnelles*, Ann. Sc. Éc. Norm. Sup., Series 3, 2, 1885, pp. 385–404.

[17] Liverani C., Turchetti G., *Improved KAM estimates for the Siegel radius*, Journal of Statistical Physics, Volume 45, Numbers 5-6, 1986, pp. 1071–1086.

[18] Markosian L., Kowalski M.A., Trychin S.J., Bourdev L.D., Goldstein D., Hughes J.F., *Real-Time Nonphotorealistic Rendering.*

[19] Milnor J.W., *Dynamics in one complex variable*, 2^{nd} edition, Vieweg, 2000.

[20] Needham T., *Visual complex analysis*, Oxford Press, 2000.

[21] Peitgen H.-O., Jürgens H., Saupe D., *Chaos and Fractals*, Springer & Verlag, 1991.

[22] Pérez-Marco R., *Fixed points and circle maps*, Acta Mathematics, 179, 1997.

[23] *The Science of Fractal Images*, edited by Heinz-Otto Peitgen and Dietmar Saupe, Springer-Verlag, New York, 1988.

[24] Rosa A., *Methods and applications to display quaternion Julia sets*, Electronic Journal of Differential Equations and Control Processes, St. Petersburg, 4, 2005, pp. 1–22.

[25] Rosa A., *On a solution to display non-filled-in quaternionic Julia sets*, arXiv cs.GR/0608003.

[26] Rosa A., *The accessibility locus theory and its applications to iterates of polynomials in one complex variable*, in preparation.

[27] Schröder E., *Über unendlich viele Algorithmen zur Auflösung der Gleichungen*, Math. Ann., 2, 1870, pp. 317–365.

[28] Schröder E., *Über iterirte Funktionen*, Math. Ann., 3, 1871, pp. 296–322.

[29] Yoccoz J.C., *Linéarisation des germes de difféomorphismes holomorphes de* $(\mathbb{C}, 0)$, Comptes Rendus Acad. Sci. Paris, Sér. I Math **306**, 1988, pp. 55–58.

[30] Yoccoz J.C., *Recent developments in dynamics*, Proceedings of the International Congress of the Mathematicians in Zürich, Birkhäuser Verlag, 1994.

[31] Zakeri S., *Dynamics of cubic Siegel polynomials*, Communications in mathematical physics (Commun. math. phys.), Springer, 1999, vol. 206, no1, pp. 185–233.